Dalton
www.rsc.org/dalton

Electronic coupling between molybdenum or tungsten quadruple bonds linked by dicarboxylate ligands †

Malcolm H. Chisholm*
Department of Chemistry, The Ohio State University, 100 West 18th Avenue, Columbus, OH 43210-1185, USA

Received 23rd June 2003, Accepted 1st August 2003
First published as an Advance Article on the web 6th September 2003

The preparations and structures of dicarboxylate bridged complexes having MM quadruple bonds are described where M = Mo or W. The electronic structure of these complexes is shown to be dramatically altered by M_2 δ-bridge π orbital interactions. The significance of M_2 δ-bridge π conjugation is revealed by electronic structure calculations employing density functional theory and is manifest in the attendant spectroscopies of these compounds (UV-vis, Raman and resonance Raman), together with electrochemical studies and the EPR spectra of the single electron oxidized radical cations.

Upon reflection, it is truly amazing to contemplate the changes in chemistry that have occurred in the 200 years since Dalton's formulation of atomic weights of the elements.[1] The latter half of the 20th century will surely be remembered as the golden age of molecular synthesis resulting from an appreciation of reaction mechanisms and electronic structure, aided by the rapid advances in spectroscopic, analytical and computational techniques. At this time, it would seem difficult to speculate about the future state of chemistry in 20 years, let alone 200 years. This notwithstanding, it seems likely that chemists will continue to synthesize new molecules and will be the architects of materials of ever increasing complexity and sophistication. Chemists are truly the molecular engineers of the future. In this Celebration Perspective, I recount efforts in this and other laboratories aimed at developing molecular assemblies incorporating metal–metal multiple bonds.

By 1990, it was well established that complexes with MM multiple bonds had a rich molecular chemistry and showed unique reactivity as a result of the presence of a redox-active, dinuclear template. Surely too, there would be a fascinating supramolecular and macromolecular chemistry? We attempted to incorporate MM quadruple bonds into one-dimensional polymers and into liquid crystalline phases.[2] We showed that the dimetal tetracarboxylates of molybdenum and tungsten, $M_2(O_2CR)_4$, could form discotic mesophases that could be aligned in a magnetic field.[3] The mesophases displayed interesting non-linear viscoelastic properties that could be related to weak intermolecular M ⋯ O bonding.[4] In the preparation of oligomeric complexes, we were also attracted to the $M_2(O_2CR)_4$ family of compounds because the carboxylates are substitutionally labile and because solubility can be influenced significantly by the choice of R group.

Syntheses and structures

The reactions between $M_2(O_2CBu^t)_4$ and dicarboxylic acids HOOC–X–COOH, gave oligomeric compounds, which were difficult to characterize and not discrete as a result of partial substitution and the occurrence of *cis* and *trans* substitution. We were, however, able to isolate and characterize a number of bridged tetranuclear complexes.[5] Ligand bridges such as 2,7-dioxynaphthyridine and anthracene-1,8-dicarboxylate afford tetranuclear chain complexes having alternating MM quadruple bonds, M–M ~2.1 Å and M ⋯ M distances of *ca* 3.0 Å, whereas the use of oxalate, anthracene-9,10-dicarboxylate and perfluoroterephthalate give tetranuclear complexes where the M_2 units are well separated and not necessarily in the same plane.

Since this initial work, others have made numerous dicarboxylate bridged compounds of the form $L_nM_2bridgeM_2L_n$ where the metal atoms, M, are Rh, Ru, Re and Mo, along with molecular triangles $[L_nM_2(bridge)]_3$ and molecular squares $[L_nM_2(bridge)]_4$.[6–14] Most notable in this regard has been the

† The above illustration of John Dalton (reproduced courtesy of the Library and Information Centre, Royal Society of Chemistry) marks the 200th anniversary of his investigations which led to the determination of atomic weights for hydrogen, nitrogen, carbon, oxygen, phosphorus and sulfur.

Malcolm H. Chisholm

Malcom H. Chisholm was born in Bombay, India (1945) to Scottish parents and educated in England, Canford School and Queen Mary College, London. He received his PhD in 1969 under the direction of Professor D. C. Bradley and did post-doctoral studies at the University of Western Ontario with Professor H. C. Clark. After academic appointments at Princeton University and Indiana University, he assumed his current position at the Ohio State University in 2000 where he is Distinguished Professor of Mathematical and Physical Sciences. His research interests include the chemistry of complexes with metal–metal multiple bonds, the use of alkoxide and related π-donor ligands in organometallic chemistry, molecular routes to materials and the development of catalysts for the preparation of biodegradable and biocompatible polymers from readily renewable resources. He is author or coauthor of over 500 publications and has received several rewards for his research including the Awards for Inorganic Chemistry and Distinguished Service to Inorganic Chemistry of the American Chemical Society and the Centenary and Ludwig Mond Lectureships of the Royal Society of Chemistry. He is a Fellow of the Royal Society, London and the recipient of the Davy Medal. He has served as Associate Editor for the Americas for Chemical Communications *and* Dalton Transactions.

DOI: 10.1039/b307167g

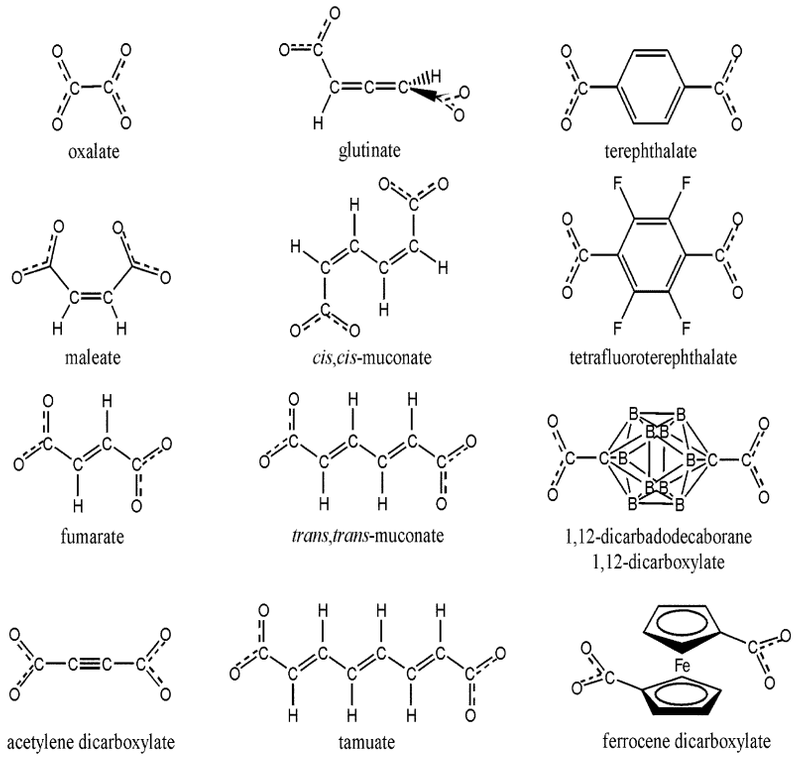

Fig. 1 Dicarboxylate ligands used to unite M_2 metal centers.

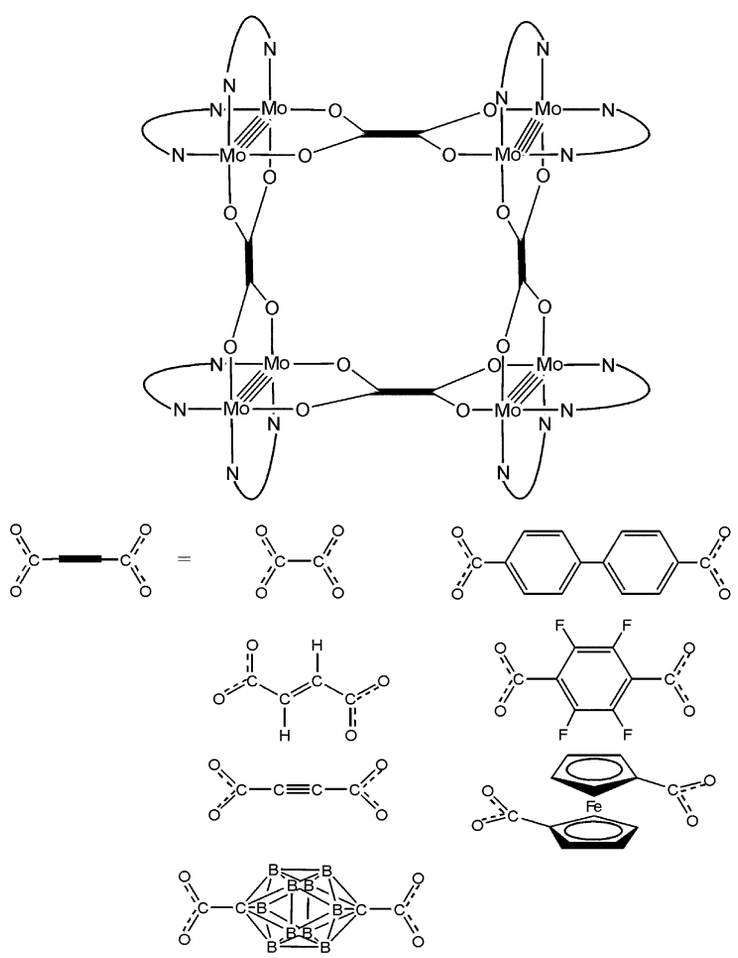

Fig. 2 Dicarboxylate bridged [Mo_2] squares (Cotton *et al.*[12,13]).

elegant synthesis and structural work of Cotton *et al.*[11–12] and representative examples are shown in Figs. 1 and 2. Their synthetic approach involved metathetic reactions of the type indicated by eqns. (1) and (2), where L = diarylformamidinate ligands.

The advantages of utilizing attendant formamidinate ligands

$$2[L_3Mo_2(CH_3CN)_2^+BF_4^-] + Na_2 \text{ bridge} \longrightarrow [L_3Mo_2]_2 \text{ bridge} + 2NaBF_4 + 2CH_3CN \quad (1)$$

$$4[L_3Mo_2Cl_2] + 2Zn + 2 \text{ Zn bridge} \longrightarrow [L_8Mo_8(\text{bridge})_4] + 4ZnCl_2 \quad (2)$$

relative to carboxylate are twofold. (1) They are notably less labile to intermolecular ligand scrambling and (2) the *trans*-influence of nitrogen is greater than that of oxygen which favors *cis*-coordination about the dinuclear center and thereby the formation of molecular squares. In the case of carboxylate and dicarboxylate ligands, there is no significant site preference about the dinuclear center. Also, even for simple dicarboxylate-linked M_2 quadruply-bonded complexes supported by pivalate ligands, the products are formed as microcrystalline powders from hydrocarbon solutions in which they are only very sparingly, if at all, soluble. In the solid state, they form coordination polymers wherein each tetranuclear molecule is associated with its neighbors through the agency of intermolecular M ⋯ O bonds.

By the use of powder X-ray diffraction studies and the application of recently developed programs, we have been able to determine the overall solid-state extended structures of certain compounds.[15] This method involves assignment of the unit cell and space group and the assumption of a reasonable molecular model for the fundamental tetranuclear unit. Given the now well-documented paddle-wheel $M_2(O_2C)_4$ central unit in molybdenum and tungsten tetracarboxylates, one can reasonably assume that this is present in these linked M_2-containing complexes. The two key uncertainties concern (1) the orientation of one M_2 unit with respect to its dicarboxylate linked partner and, (2) how each tetranuclear complex is coordinated to neighboring molecules in the solid state. In the case of the oxalate bridged complexes, the first question concerns the torsion angle about the central oxalate C–C bond, but in the case of a bridge such as terephthalate or anthracene-9,10-dicarboxylate, the relative orientation of the planar phenyl or anthracenyl ring needs to be determined. The second matter of how each M_4 molecule is coordinated to its neighbors can only be deduced easily if there is a small number of subunits in the unit cell.

The best fit of the calculated and the observed diffraction pattern data for $[Mo_2(O_2C^tBu)_3]_2(\mu\text{-}O_2CCO_2)$ indicated a near planar oxalate ligand having a O–C–C–O torsion angle $\theta \sim 10°$ where $\theta = 0°$ is rigorously planar. In the solid state, each Mo_4 unit is connected to its nearest neighbors through the use of both oxalate and pivalate oxygen atoms, forming an infinite chain of Mo_4-containing molecules as shown schematically in **A**.[15]

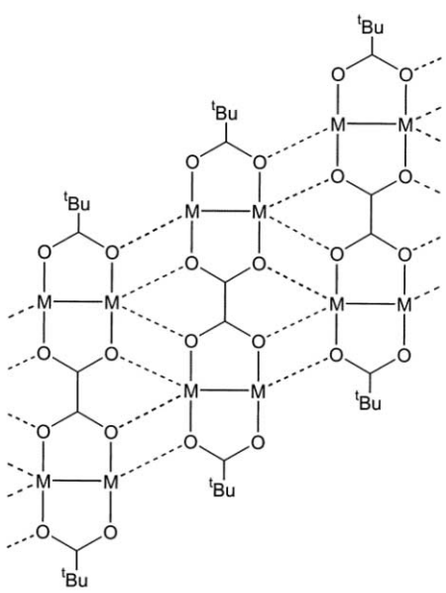

A

This type of extended structure is only possible for oxalate, although all dicarboxylate-bridged structures can form laddered structures from each M_2 unit *via* $M_2 \cdots O$ intermolecular bonding. The perfluoroterephthalate complex $[(^tBuCO_2)_3Mo_2]_2(\mu\text{-}O_2CC_6F_4CO_2)$ was shown by powder X-ray diffraction studies to adopt the polymeric structure shown in **B**.[15] Here the two Mo_2 units in the same molecule are not in the same plane but are twisted with a θ angle of 54°. Moreover, the blade of the phenyl group is twisted nearly 90° from one MoMo axis and, as we shall show later, this removes electronic communication between the two dicarboxylate-linked M_2 centers.

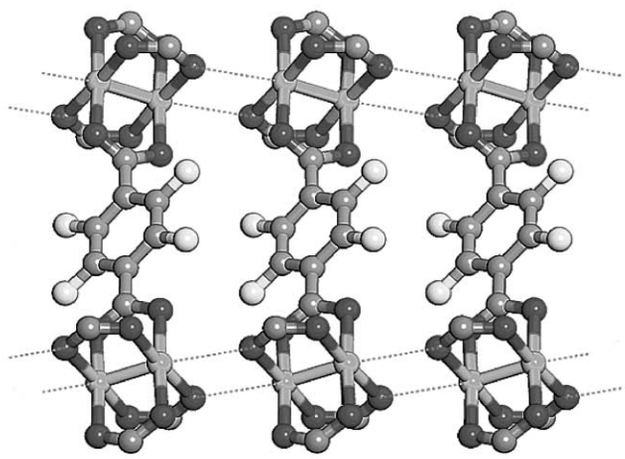

B

Electrochemical studies

A simple measure of the electronic coupling between the two dinuclear metal centers was gleaned from electrochemical studies involving cyclic voltammetry and differential pulsed voltammetry.[5] When the metal atoms are aligned in a chain, as in the 2,7-dioxynaphthyridine or anthracene-1,8-dicarboxylate linked compounds, the central metal atoms are *ca* 3.0 Å apart, but the $\Delta E_{1/2}$ values, the difference between the first and second oxidation potentials, are very sensitive to the nature of the bridge. See Table 1. It thus follows that the electronic coupling is through the bridge. Based on the magnitude of $\Delta E_{1/2}$, one can determine the comproportionation constant, K_c, for eqn. (3) shown below,[16] and based on the magnitude of K_c, these mixed-valence complexes may be categorized according to the Robin and Day Scheme where Class I corresponds to valence trapped, Class III to fully delocalized and Class II to strongly coupled.[17]

$$[M_2 \sim\sim M_2] + [M_2 \sim\sim M_2]^{2+} \rightleftharpoons 2[M_2 \sim\sim M_2]^+, K_c \quad (3)$$

A close similarity with the Taube pentamine ruthenium and osmium bridged complexes $[(NH_3)_5M(\text{bridge})M(NH_3)_5]^{4/5/6+}$ can be seen for which the K_c values are notably larger for the 3rd row transition element Os relative to Ru.[16] Also, K_c decreases with increasing distance between the metal centers and this was very nicely seen in a recent study by Cotton *et al.* for a series of $O_2C(CH{=}CH)_nCO_2$ bridged Mo_2 complexes where n = 1, 2, 3 and 4.[14] Another indication of strongly coupled M_2 centers is seen in the relative ease of oxidation of the bridged tetranuclear complexes relative to the parent $M_2(O_2C^tBu)_4$ complex. For example, the first oxidation potential for the oxalate bridged tungsten complex $[(^tBuCO_2)_3W_2]_2(\mu\text{-}O_2CCO_2)$ is at −1.26 V relative to $Cp_2Fe^{o/+}$ which may be compared to −0.70 V for the parent compound $W_2(O_2C^tBu)_4$.

When the ligand bridge is itself electrochemically oxidizible or reducible, the redox chemistry can be even more interesting.

Table 1 Comparison of electrochemical oxidation potentials[a] for various linked and unlinked MM quadruply bonded complexes with pivalate ligands referenced to $[Cp_2Fe]^{0/+}$

Compound	$E_{½}^{1}$/V	$E_{½}^{2}$/V	$\Delta E_{½}^{1,2}$/mV
$[\{Mo_2(O_2C^tBu)_3\}_2(\mu\text{-}9,10\text{-}An(CO_2)_2)]$[b]	+0.04	+0.10	60
$[\{W_2(O_2C^tBu)_3\}_2(\mu\text{-}9,10\text{-}An(CO_2)_2)]$[b]	−0.62	−0.53	90
$[\{Mo_2(O_2C^tBu)_3\}_2(\mu\text{–}C_2O_4)]$[c]	−0.03	+0.25	280
$[\{W_2(O_2C^tBu)_3(\mu\text{–}C_2O_4)]$[c]	−1.26	−0.54	717
$[\{Mo_2(O_2C^tBu)_3\}_2(\mu\text{-}1,4\text{-}C_6F_4(CO_2)_2)]$[c]	+0.10		65[d]
$[\{W_2(O_2C^tBu)_3\}_2(\mu\text{-}1,4\text{-}C_6F_4(CO_2)_2)]$[c]	−0.66	−0.37	285
$[\{W_2(O_2C^tBu)_3\}_2(\mu\text{-}1,8\text{-}An(CO_2)_2)]$[c]	−0.66	−0.51	156
$[\{W_2(O_2C^tBu)_3\}_2(\mu\text{-}1,1'\text{-}Fe(\eta^5\text{-}C_5H_4CO_2)_2)]$[c]	−0.62	−0.53	90
$[Mo_2(O_2C^tBu)_4]$[c]	−0.04		
$[W_2(O_2C^tBu)_4]$[c]	−0.70		

[a] $E_{½}^{1}$ and $E_{½}^{2}$ values correspond to E_p^{1} and E_p^{2}, respectively. [b] Ref. 28. [c] Ref. 29. [d] Estimated, see ref. 29.

In the case of oxidation, the EPR spectrum of the radical cation can establish unequivocally whether or not oxidation is metal centered. A similar situation pertains for reduction and, in the cases we have encountered, the reduction of the bridge can be reliably gauged by the behavior of the reduction wave of the bridging ligand itself. The bridging ligands 9,10-anthracenedicarboxylate, for example, and 2,5-thiophenedicarboxylate show quasi-reversible reduction waves at *ca.* −2 V *versus* $Cp_2Fe^{o/+}$ couple in tetrahydrofuran.

Electronic structure calculations

Molecular orbital calculations employing density functional theory with commercially available programs provided by Gaussian 98 and ADF 2000 on model compounds where formate substitutes for pivalate have provided remarkably good insight into the electronic structure of these dicarboxylate-bridged complexes.[18,19] These computational methods simulate the observed solid-state molecular structure parameters and reproduce vibrational and electronic absorption spectra remarkably well. They also allow one to interrogate the bonding in molecules having different conformations. Despite the power of these modern computational methods, it is heartening that relatively elementary considerations of symmetry and bonding provide the essential insight into the origins of the electronic coupling and the magnitude of these interactions.

For oxalate, the important orbital interactions that couple the two dinuclear centers arise from the interactions of the M_2 δ and CO_2 π orbitals shown pictorially in **C** and **D** below.

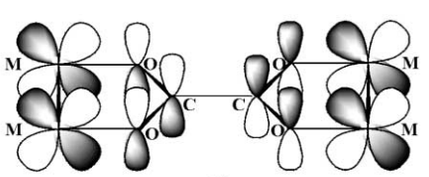

C

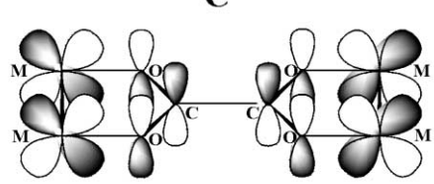

D

In **C**, the filled out-of-phase combination of M_2 δ orbitals interacts with a filled CO_2 π bonding orbital which result in a destabilization of the out-of-phase M_2 δ combination. In **D**, the in-phase δ interacts with the LUMO of the oxalate dianion. This is a filled–empty orbital interaction and leads to a stabilization of the in-phase M_2 δ orbital. It also places electron density in a C–C π bonding molecular orbital of the oxalate bridge and thus favors a planar oxalate bridge. The degree of this M_2 δ to $C_2O_4^{2-}$ back bonding depends on the relative energies of the M_2 δ orbitals and consequently the tungsten complexes are more strongly coupled compared to their molybdenum analogues. See Table 1. For related complexes, the W_2 δ orbitals are 0.5 eV higher in energy than their Mo_2 δ orbital counterparts.[20]

Based on the electronic structure calculations on the model compounds $[(HCO_2)_3M_2]_2(\mu\text{-}O_2CCO_2)$, the planar D_{2h} structure is favored by *ca.* 8 kcal mol^{-1} for tungsten and 5 kcal mol^{-1} for molybdenum.[21] In the planar structure, the splitting of the M_2 δ combinations is approximately 0.5 eV for tungsten and 0.3 eV for molybdenum. These M_2 δ combinations are the HOMO and HOMO-1 orbitals, while the LUMO is oxalate-centered. The HOMO–LUMO electronic transition is a fully-allowed MLCT transition. The relative energies of these three molecular orbitals, the HOMO-1, HOMO and LUMO are very sensitive to the torsion angle about the C–C bond of the oxalate. Probably the simplest way to show this is by way of the MO pictorial energy level diagram connecting the orbitals of the planar D_{2h} $[(HCO_2)_3W_2]_2(\mu\text{-}O_2CCO_2)$ molecule, θ = 0°, with the D_{2d} structure, θ = 90°. See Fig. 3.

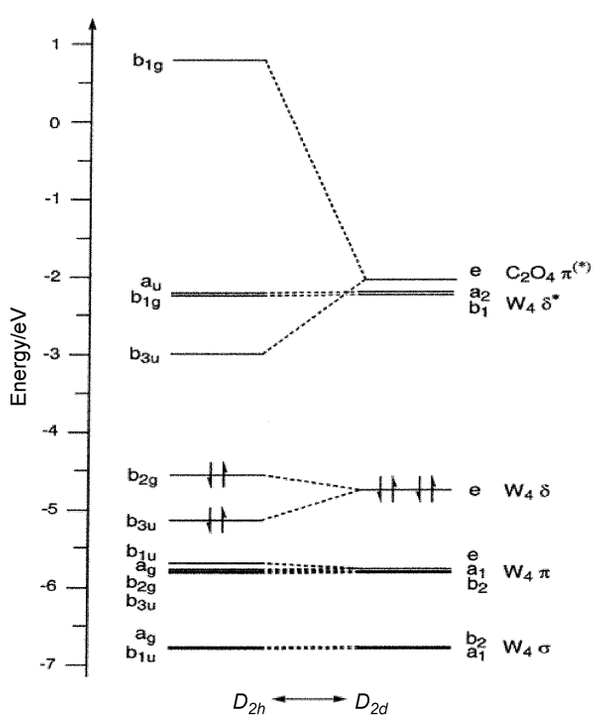

Fig. 3 Correlation MO energy level diagram for planar and twisted (D_{2h} *vs.* D_{2d}) $[(HCO_2)_3(M_2)]_2(\mu\text{-}O_2CCO_2)$.

The HOMO–LUMO gap changes from *ca.* 1.5 to 3.0 eV as θ goes from 0° to 90° and in D_{2d} symmetry, the two M_2 δ orbitals are degenerate. The electronic coupling is thus very sensitive to

the C–C torsion angle and these compounds show interesting thermochromism in solution which will be described later. The oxalate-bridged compounds also show an increase in the $\Delta E_{1/2}$ values, the separation of the 1st and 2nd oxidation waves in their cyclic voltammograms, upon lowering the temperature. This can be correlated with the energy separation of the HOMO and HOMO-1.

Based on an understanding of the oxalate-bridged compounds, one can readily anticipate the key orbital interactions that arise for other conjugated dicarboxylates, $[O_2C–X–CO_2]^{2-}$, such as acetylene dicarboxylate, perfluoroterephthalate and 2,5-thienyldicarboxylate.[19,23] In all cases, the in-phase M_2 δ combination allows for a mixing with the LUMO of the planar bridge. This is the key orbital interaction leading to the electronic coupling of the two dinuclear centers. Based on the coupling of two dinuclear centers *via* a $[O_2C–X–CO_2]^{2-}$ bridge, we can also start to anticipate the nature of the bonding in extended chains and in molecular squares and triangles.

For a one-dimensional chain of oxalate-bridged dimetal species $[M_2]_n(oxalate)_{n-1}$, the M_2 δ orbital combinations are $n/2$ b_{2g} and $(n-1)/2$ b_{3u} where n is odd in D_{2h} symmetry. The empty oxalate-bridged orbitals are $(n-2)/2$ b_{2g} and $n/2$ b_{3u} when n is even and $(n-1)/2$ b_{2g} and $(n-1)/2$ b_{3u} when n is odd. In an infinite chain, the M_2 δ combinations form the filled valence δ band and the oxalate π* orbitals the empty conduction band.

For the molecular square, the four M_2 δ combinations comprise MOs of b_{2g}, e_u and a_{1g} symmetry in the point group D_{4h}. The vacant oxalate π orbitals transform as a_{1g}, e_u and b_{1g}. In both the linear chain and square molecules, there is little orbital mixing between the M_2 units and the oxalates other than those of the M_2 δ's and the oxalate filled and vacant orbitals shown in **C** and **D**. The MM π, π* and δ* orbitals do not find suitable partners with the oxalate. Thus the quadruply-bonded complexes of molybdenum and tungsten are predicted to be those complexes most suitable for this type of electronic coupling. The molecular orbital plots for the frontier MOs of the oxalate-bridged chain compound $(HCO_2)_{10}M_8(O_2CCO_2)_3$ and the molecular square $(HCO_2)_8M_8(O_2CCO_2)_4$ are shown in Fig. 4. From these orbital plots, it is readily apparent that the metal centers are strongly coupled as a result of M_2 δ ligand bridge πconjugation.

For a bridge such as $[O_2CCH=C=CHCO_2]^{2-}$, where the two CO_2 units are at right angles, the coupling is lost.[14] For the 9,10-anthracenedicarboxylate bridged complex, which as a result of the opposing electronic and steric factors (unfavorable CH ⋯ O interactions) adopts a twisted D_2 structure with a 54° dihedral angle between the CO_2 plane and that of the anthracene ring, the electronic coupling is muted.[23]

Electronic absorption spectra

The dicarboxylate bridged compounds which have strongly coupled dinuclear centers are intensely colored as a result of M_2 δ to bridge π* electronic transitions. For the same bridge, the electronic absorption bands in the visible region are red shifted and notably more intense for tungsten complexes relative to molybdenum. This is entirely consistent with the fact that the W_2 δ orbitals are higher in energy and thus closer in energy to the LUMO of the bridge. Moreover, to a first approximation, the intensity of a fully allowed metal–ligand charge transfer transition correlates with the orbital overlap. The colors of the compounds are also very sensitive to their phase and many show marked solvatochromism.[22] Examples of the room temperature spectra of $[(^tBuCO_2)_3W_2]_2(\mu\text{-}O_2CCO_2)$ recorded in various solvents are shown in Fig. 5.

These very intense absorptions show evidence of a vibronic progression associated with the totally symmetric oxalate ν_1 and ν_2 modes of the photoexcited state molecule (see later). Upon lowering the temperature in 2-methyltetrahydrofuran which forms a glass at ~ −140 K, there is a pronounced bathochromic shift and at 2 K vibronic progressions, one in 1550 cm^{-1} and the other in 800 cm^{-1}, are well resolved. The red shift in the oxalate spectrum is entirely consistent with expectations that the ground state planar geometry is favored as thermal energy decreases. As $T \longrightarrow 2$ K, the Boltzmann distribution of molecules having $\theta \longrightarrow 0°$ increases. The appearance of the vibronic features is understandable in terms of the molecular orbital analysis presented earlier. In the photoexcited state, an electron is placed in the LUMO and this is almost exclusively centered on the oxalate bridge with C–C π bonding and C–O π* antibonding character. We therefore expect a significant change in oxalate atomic positions upon excitation from the ground state to the first photoexcited state.

A comparison of the electronic absorption spectra of the 2,5-thienyldicarboxylate molybdenum and tungsten pivalate compounds is shown in Fig. 6. These reveal similar trends. The low energy absorptions arise from M_2 δ to bridge π* MLCT transitions which are notably more intense and at lower energy for the tungsten complex relative to molybdenum. Once again, there is a vibronic progression in the case of the tetranuclear tungsten complex and upon lowering the temperature in a 2-methyltetrahydrofuan glass, there is a significant red shift and the vibronic features become more pronounced.

The greatest thermochromic behavior in solution and in a glass is seen for the perfluoroterephthalate bridged tungsten complex $[(^tBuCO_2)_3W_2]_2(\mu\text{-}O_2CC_6F_4CO_2)$ which, as shown in Fig. 7, shifts an absorption in the visible region of the spectrum at room temperature well into the near IR upon cooling. The calculated energy favoring the all-planar, D_{2h} structure, which allows for maximum electronic coupling, is *ca.* 3–5 kcal mol^{-1}, and the HOMO–LUMO MLCT transition is very sensitive to the relative orientation of the phenyl ring.[24]

Resonance Raman spectroscopy

With excitation into the intense absorption bands in the visible region of the electronic spectrum, many of these compounds show remarkable resonance enhancements of Raman bands associated with the totally symmetrical vibrations of the bridging dicarboxylates, the MM stretching mode and overtones and combinations of these bands. This is very clearly illustrated by the resonance Raman spectra of the oxalate bridged compounds which show pronounced resonance enhancement of ν_1, ν_2 and ν_3 of the oxalate, formally assignable to νCO_2, νCC and δCO_2, together with ν(MM) and several combinations and overtones.[21] The DFT calculations on the model compound $[(HCO_2)_3Mo_2]_2(\mu\text{-}O_2CCO_2)$ indicated that for the planar D_{2h} structure there is very extensive mixing of the CO_2 and C–C stretching modes and that even δCO_2 and νCC are mixed. A comparison of the observed and calculated Raman data is given in Table 2. Given that the electronic transition that is responsible for this resonance enhancement involves an M_2 δ-to-oxalate π* transition, we anticipate that the most significant change in geometry involves the C–C and C–O bond distances of the oxalate and, to a lesser extent, the MM distance (as noted before). Consequently, these vibrational modes show the most resonance enhancement.

The vibronic progressions in electronic absorption spectra are also understood in terms of the nature of the M_2 δ to bridge π* transition. These progressions arise from totally symmetric vibrations of the ligand bridge in the photoexcited state molecule. As can be seen from an inspection of Fig. 8, the labeling of the oxalate bridge $O_2{}^{13}C{}^{13}CO_2$ causes a pronounced isotopic shift in the progression of ν_1 for the excited state molecule, again implying extensive mixing of the νCO_2 and νCC modes of oxalate in the photoexcited state.

Radical cations

While a great deal can be inferred about the degree of electronic coupling in dicarboxylate complexes in their neutral states, the

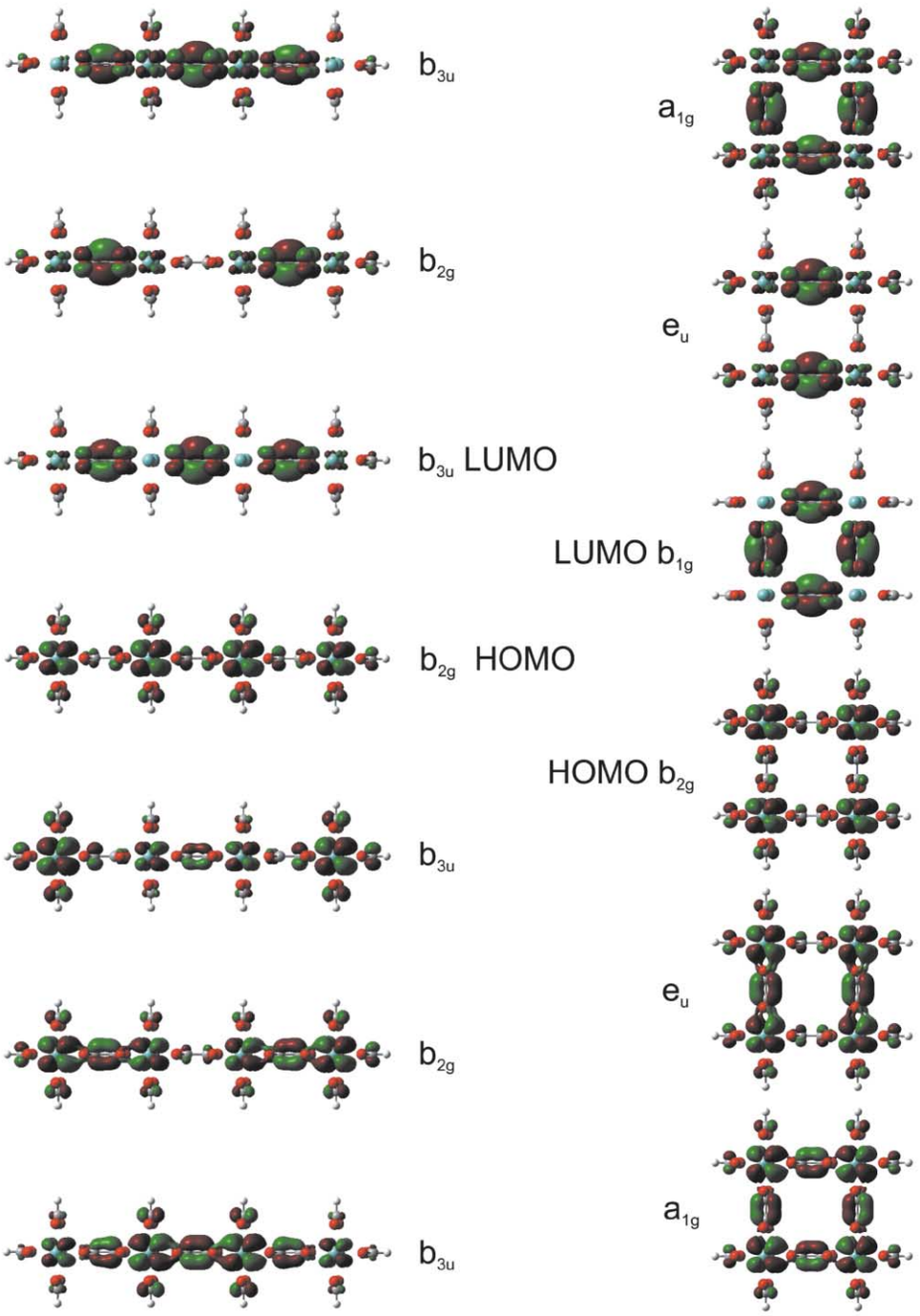

Fig. 4 Frontier orbitals of D_{2h} (chain) and D_{4h} (square) $[M_2]_4$ oxalate bridged complexes supported by formate ligands.

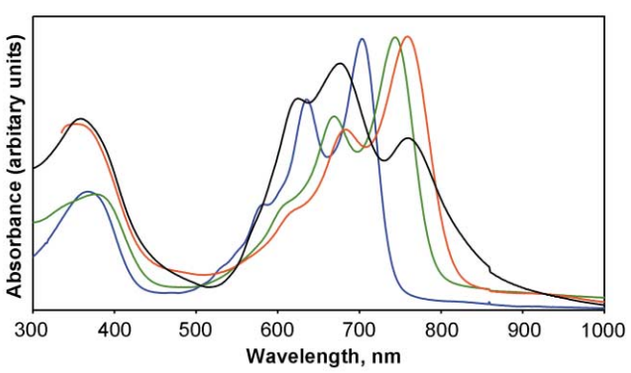

Fig. 5 Room temperature visible spectrum of $[(^tBuCO_2)_3W_2]_2$-(μ-O_2CCO_2) in various solvents. In water (black), THF (blue), DMSO (green) and aniline (red).

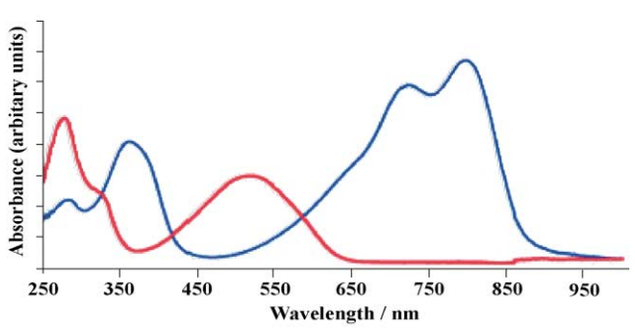

Fig. 6 Comparison of the visible region of the electronic absorption spectra for $[(^tBuCO_2)_3M_2]$(μ-2,5-thienyldicarboxylate) where M = Mo and W in THF.

Table 2 Vibrational data for $[(^tBuCO_2)_3Mo_2]_2(\mu\text{-}O_2CCO_2)$ and that calculated for $[(HCO_2)_3Mo_2]_2(\mu\text{-}O_2CCO_2)$

band	Mo_4OXA_{obs} ν/cm^{-1}	$Mo_4\,^{13}C\text{–}OXA_{obs}$ ν/cm^{-1}	Δ_{obs} ν/cm^{-1}	Mo_4OXA_{calc} ν/cm^{-1}	$Mo_4\,^{13}C\text{–}OXA_{calc}$ ν/cm^{-1}	Δ_{calc} ν/cm^{-1}
ν_1	1411	1367	−44	1423	1380	−43
ν_2	932	927	−5	945	938	−7
ν_3	576	573	−3	584	583	−1

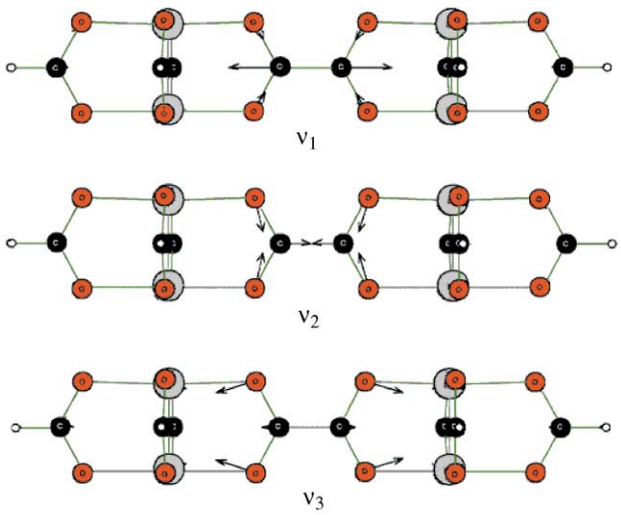

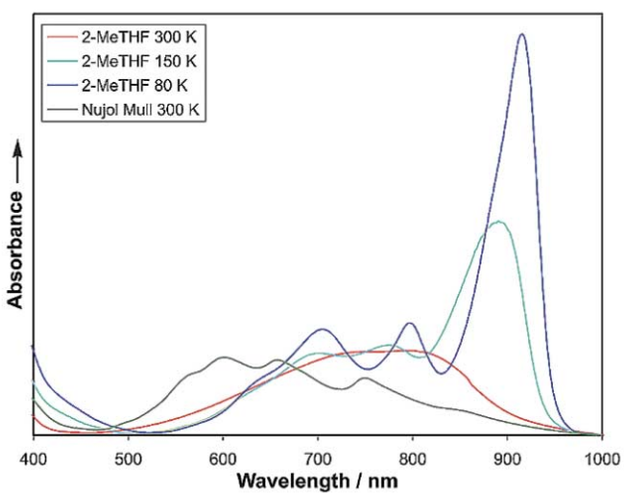

Fig. 7 Comparison between the Nujol Mull and various temperature 2-MeTHF spectra of $[(^tBuCO_2)_3W_2]_2(\mu\text{-}O_2C_6F_4CO_2)$.

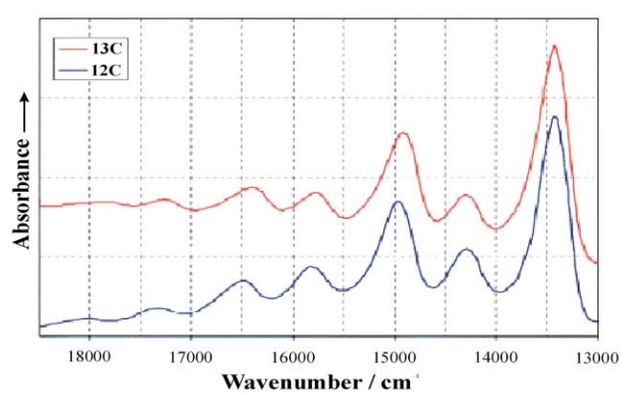

Fig. 8 Low temperature, 2 K electronic absorption spectra of $[(^tBuCO_2)_3W_2](\mu\text{-}O_2{*}C{*}CO_2)$, where *C = ^{12}C or ^{13}C, recorded in 2-MeTHF.

one-electron oxidized radical cations provide an opportunity to explore the degree of electron delocalization in the formally mixed valence systems. Oxidation of $M_2(O_2CR)_4$ compounds produces the radical cations with MM bond order of 3.5 and a MM bonding electronic configuration $\sigma^2\pi^4\delta^1$. These compounds show electronic transitions due to $\delta^1\delta^{*\circ} \longrightarrow \delta^\circ\delta^{*1}$ and EPR signals due to the presence of the unpaired electron in the δ orbital which is axially symmetric. Both molybdenum and tungsten have certain nuclei that are spin active: $^{97/95}$Mo, $I = 5/2$, $\Sigma I = 25\%$ and ^{183}W, $I = 1/2$, 14.5% natural abundance. The isotropic EPR spectra of $M_2(O_2CR)_4^+$ radical cations show a central signal for which g is less than 2 due to spin–orbit coupling (this is most pronounced for tungsten due to very large spin–orbit coupling), flanked by a hyperfine spectrum due to the presence of the magnetically-active nuclei. The oxidized dicarboxylate-linked dinuclear compounds can appear on the EPR timescale as valence trapped, where only one M_2 unit is oxidized, or as fully delocalized where the description $[M_4]^+$ is appropriate.[25] In our hands, we have experienced both limiting situations and, for a given bridge, the tungsten complexes show greater delocalization in their radical cations. For example, the cations $[(^tBuCO_2)_3M_2]_2$(μ-2,5-thienyldicarboxylate)$^+$ formed from the reaction between the neutral dicarboxylate complexes and $Cp_2Fe^+PF_6^-$ in THF/CH_2Cl_2, show EPR spectra consistent with valence trapped for M = Mo and delocalized for M = W.[26] See Fig. 9. The isotropic spectrum for the molybdenum complex closely parallels that for $Mo_2(O_2CBu^t)_4^+$ while the tungsten complex shows a lower g value than $W_2(O_2C^tBu)_4^+$ and a notably smaller hyperfine coupling constant to ^{183}W. This parallels the behavior of radical Mo(bridge Mo)$_n$ containing species which show smaller values of A_o as n increases from 1 to 2 as reported by McCleverty and Ward.[27]

As noted earlier, the electronic coupling is very sensitive to torsion angles and, for certain ligand bridges, it appears that we observe temperature-dependent EPR spectra corresponding to equilibrium mixtures of valence trapped and delocalized species on the EPR timescale.[23]

The timescale of the EPR experiment, although fast ~10^{-10} s, is not as fast as the timescale of electronic or vibronic transitions and we have, therefore, started to study the resonance Raman spectra and electronic absorption spectra of these radical cations. Many of the strongly-coupled complexes show low-energy electronic absorption bands in the near IR.[22] For fully delocalized systems, those for which the half width of the bands are less than 2310 cm^{-1}, these transition energies, E_{op}, provide a

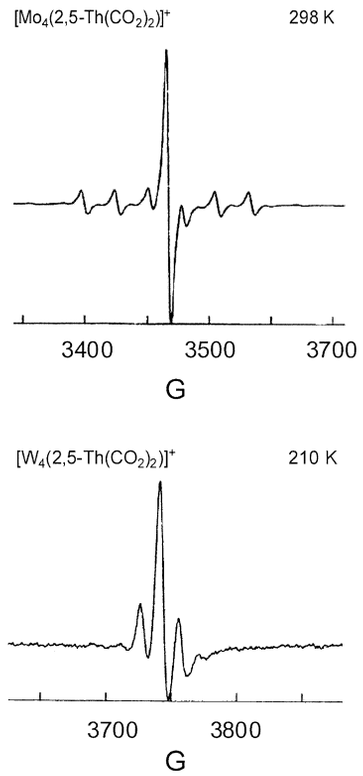

Fig. 9 EPR spectra of $[(^tBuCO_2)_3M_2]_2$(μ-2,5-thienyldicarboxylate) where M = Mo or W.

direct measure of the electronic coupling, $2H_{AB}$. For the oxalate bridged radical cations, H_{AB} = 2980 and 2000 cm^{-1} for M = W and Mo, respectively. As the bridge gets longer, as in perfluoroterephthalate and 2,5-thienyldicarboxylate, the values of H_{AB} decrease and we observe Class II behavior. Based on the earlier discussion, these low energy bands are expected to show a significant temperature dependence, both in the position of λ_{max} and in $\Delta\bar{\nu}$. This topic is currently under investigation, but it is already clear from preliminary studies of the spectroscopy associated with these radical cations that the electron delocalization is greatly dependent on the nature of the bridge and, for any specific bridge, is always greater for tungsten relative to molybdenum.

Concluding remarks

M_2 δ-to-bridge π-conjugation provides the mechanism for electronically coupling MM quadruple bonds. The degree of coupling is dependent on the relative energies of the M_2 δ orbitals and the π-system of the dicarboxylate bridge. The coupling is attenuated by distance and by torsion angles. This leads to thermo- and solvato-chromism and the potential for molecular switching and signaling. Electronically-coupled MM multiply-bonded complexes with redox-active metal centers thus provide fascinating possibilities as building blocks for higher order assemblies of inorganic–organic hybrid materials.

Acknowledgements

I thank my talented coworkers and collaborators who are cited in the references and the National Science Foundation for support of this work.

References

1 M. F. Lappert, *Dalton Trans.*, 2003, DOI: 10.1039/b307622a.
2 M. H. Chisholm, *Acc. Chem. Res.*, 2000, **33**, 53.
3 D. V. Baxter, R. H. Cayton, M. H. Chisholm, J. C. Huffman, E. F. Putilina, S. L. Tagg, J. L. Wesemann and J. W. Zwanziger, *J. Am. Chem. Soc.*, 1994, **116**, 4551–4566.
4 M. R. Mackley, R. T. J. Marshall, M. H. Chisholm and E. F. Putilina, *Chem. Mater.*, 1995, **7**, 1938–1941.
5 R. H. Cayton, M. H. Chisholm, J. C. Huffman and E. B. Lobkovsky, *J. Am. Chem. Soc.*, 1991, **113**, 8709–8724.
6 R. P. Bonar-Law, T. D. McGrath, N. Singh, J. F. Buckley and A. Steiner, *Chem. Commun.*, 1999, 2457.
7 R. P. Bonar-Law, T. D. McGrath, J. F. Bickely, C. Fermoni and A. Steiner, *Inorg. Chem. Commun,.*, 2001, **4**, 16.
8 R. P. Bonar-Law, T. D. McGrath, N. Singh, J. F. Bickley, C. Fermoni and A. Steiner, *J. Chem. Soc., Dalton Trans.*, 2000, 4343.
9 J. F. Bickley, R. P. Bonar-Law, C. Fermoni E. J. MacLean, A. Steiner and S. J. Teat, *J. Chem. Soc., Dalton Trans.*, 2000, 4025.
10 J. K. Bera, R. Clerac, P. E. Fanwick and R. A. Walton, *J. Chem. Soc., Dalton Trans.*, 2002, 2168.
11 F. A. Cotton, C. Lin and C. A. Murillo, *Proc. Natl. Acad. Sci.*, 2002, **99**, 4810.
12 F. A. Cotton, C. Lin and C. A. Murillo, *Acc. Chem. Res.*, 2001, **34**, 759.
13 F. A. Cotton, J. P. Donahue, C. A. Murillo and C. M. Perez, *J. Am. Chem. Soc.*, 2003, **125**, 5496.
14 F. A. Cotton, J. P. Donahue and C. A. Murillo, *J. Am. Chem. Soc.*, 2003, **125**, 5436.
15 M. H. Chisholm, P. J. Wilson and P. M. Woodward, *Chem. Commun.*, 2002, 506–507.
16 D. E. Richardson and H. Taube, *Coord. Chem. Rev.*, 1984, **50**, 107.
17 M. B. Robin and P. Day, *Adv. Inorg. Radiochem.*, 1967, **10**, 247.
18 B. E. Bursten, M. H. Chisholm, C. M. Hadad, J. Li and P. J. Wilson, *Chem. Commun.*, 2001, 2382–2383.
19 B. E. Bursten, M. H. Chisholm, C. M. Hadad, J. Li and P. J. Wilson, *Isr. J. Chem.*, 2001, **41**, 187–195.
20 F. A. Cotton and R. A. Walton, *Multiple Bonds Between Metal Atoms*, Oxford University Press, 2nd edn., 1994.
21 B. E. Bursten, M. H. Chisholm, R. J. H. Clark, S. Firth, C. M. Hadad, A. M. Macintosh, P. J. Wilson, P. M. Woodward and J. M. Zaleski, *J. Am. Chem. Soc.*, 2002, **124**, 3050–3063.
22 M. H. Chisholm and N. Patmore, results to be published.
23 M. A. Byrnes and M. H. Chisholm, results to be published.
24 B. E. Bursten, M. H. Chisholm, R. J. H. Clark, S. Firth, C. M. Hadad, P. J. Wilson, P. M. Woodward and J. M. Zaleski, *J. Am. Chem. Soc.*, 2002, **124**, 12244–12254.
25 M. H. Chisholm, B. D. Pate, P. J. Wilson and J. M. Zaleski, *Chem. Commun.*, 2002, 1084–1085.
26 M. J. Byrnes and M. H. Chisholm, *Chem. Commun.*, 2002, 2040–2041.
27 J. A. McCleverty and M. D. Ward, *Acc. Chem. Res.*, 1998, **31**, 842.
28 M. A. Byrnes and M. H. Chisholm, results to be published.
29 R. H. Cayton, M. H. Chisholm, J. C. Huffman and E. B. Lobkovsky, *J. Am. Chem. Soc.*, 1991, **113**, 8709–8724.